



# Genomic characterization of circoviruses associated with acute gastroenteritis in minks in northeastern China

Junwei Ge<sup>1,3</sup> · Shanshan Gu<sup>1</sup> · Xingyang Cui<sup>1</sup> · Lili Zhao<sup>2</sup> · Dexing Ma<sup>1</sup> · Yunjia Shi<sup>1</sup> · Yuanzhi Wang<sup>2</sup> · Taofeng Lu<sup>2</sup> · Hongyan Chen<sup>2</sup>

Received: 16 January 2018 / Accepted: 26 May 2018 / Published online: 14 June 2018  
© Springer-Verlag GmbH Austria, part of Springer Nature 2018

## Abstract

Mink circovirus (MiCV), a virus that was newly discovered in 2013, has been associated with enteric disease. However, its etiological role in acute gastroenteritis is unclear, and its genetic characteristics are poorly described. In this study, the role of circoviruses (CVs) in mink acute gastroenteritis was investigated, and the MiCV genome was molecularly characterized through sequence analysis. Detection results demonstrated that MiCV was the only pathogen found in this infection. MiCVs and previously characterized CVs shared genome organizational features, including the presence of (i) a potential stem-loop/nonanucleotide motif that is considered to be the origin of virus DNA replication; (ii) two major inversely arranged open reading frames encoding putative replication-associated proteins (Rep) and a capsid protein; (iii) direct and inverse repeated sequences within the putative 5' region; and (iv) motifs in Rep. Pairwise comparisons showed that the capsid proteins of MiCV shared the highest amino acid sequence identity with those of porcine CV (PCV) 2 (45.4%) and bat CV (BatCV) 1 (45.4%). The amino acid sequence identity levels of Rep shared by MiCV with BatCV 1 (79.7%) and dog CV (dogCV) (54.5%) were broadly similar to those with starling CV (51.1%) and PCVs (46.5%). Phylogenetic analysis indicated that MiCVs were more closely related to mammalian CVs, such as BatCV, PCV, and dogCV, than to other animal CVs. Among mammalian CVs, MiCV and BatCV 1 were the most closely related. This study could contribute to understanding the potential pathogenicity of MiCV and the evolutionary and pathogenic characteristics of mammalian CVs.

Circoviruses (CVs) are small nonenveloped icosahedral viruses measuring 16–26 nm in diameter and possessing a single-stranded circular DNA genome with a length of 1.7–2.1 kb and a major structural protein [1]. In the current taxonomy release, the family *Circoviridae* is divided into two genera: *Circovirus* and *Cyclovirus* [1, 2]. The most recent release of the Universal Virus Database of the International Committee on Taxonomy of Viruses reported that

the genus *Circovirus* includes 29 recognized species whose members infect mammals and birds (ICTV, [https://talk.ictvonline.org/taxonomy/p/taxonomy-history?taxnode\\_id=20175768](https://talk.ictvonline.org/taxonomy/p/taxonomy-history?taxnode_id=20175768), Released on July 2017).

CVs have been identified in numerous species associated with various clinical disorders, including asymptomatic infections and lethal diseases [3–5]. In birds, CV infections are associated with lethargy, weight loss, respiratory distress, diarrhea, and poor race performance [6–8]. In geese, these infections cause death. In other animals, these infections induce different clinical signs, including respiratory, vesicular, hemorrhagic, and gastroenteritic manifestations and reproductive failure [3, 9]. CV infections are also related to lymphoid depletion and immunosuppression, which likely increase the severity of secondary infection [10].

Mink circovirus (MiCV) is a novel pathogen that was found in cases of minks with diarrhea in Dalian City, Liaoning Province, China, in 2013 [11]. Despite the discovery of CV infection in minks, the pathogenic role of MiCV in single or polymicrobial infections has not been determined,

Handling Editor: Roman Pogranichniy.

✉ Hongyan Chen  
chenhongyan@caas.cn

<sup>1</sup> College of Veterinary Medicine, Northeast Agricultural University, Harbin 150030, China

<sup>2</sup> Laboratory Animal and Comparative Medicine Unit, Harbin Veterinary Research Institute, The Chinese Academy of Agricultural Sciences, No. 678 Haping Rd, Harbin 150069, China

<sup>3</sup> Northeastern Science Inspection Station, China Ministry of Agriculture Key Laboratory of Animal Pathogen Biology, Harbin 150030, China

and the prevalence and economic importance of this virus have yet to be elucidated.

In this study, MiCV was detected and molecularly characterized from the collected feces of minks with acute gastroenteritis in Harbin City, Heilongjiang Province, in northeastern China in March 2015. The complete genome sequences of MiCV strains were compared with those of other CV strains, including recent CVs detected in birds and animals, to enhance our understanding of their genetic and biological differences.

In March 2015 an outbreak of acute gastroenteritis occurred on three farms under one cooperative in Harbin, Northeastern China. Minks had a sudden onset of gastrointestinal symptoms, and their clinical signs included severe diarrhea, vomiting, lethargy, anorexia, dehydration, and rough fur. Their stool was thin or soft and watery. More than 2000 minks were owned by the cooperative in the reproduction period, and the same feed and immune procedures were used. A 5-year vaccination protocol against mink enteritis virus (MEV) and canine distemper virus (CDV) was completed. Fewer than 10 minks died after 1 week of illness, and most of those that died were malnourished. The other minks completely recovered within 5–7 days after showing clinical signs. Local veterinary clinicians sampled three or five diarrheic fecal samples from each farm and immediately submitted them to our laboratory in the Animal Teaching Hospital of the College of Veterinary Medicine, Northeast Agricultural University.

One mink carcass (after flaying) was frozen at  $-20\text{ }^{\circ}\text{C}$  to  $-30\text{ }^{\circ}\text{C}$  after 2 days of storage at  $10\text{ }^{\circ}\text{C}$  and sent to our department for necropsy and laboratory investigations. Samples from the heart, liver, spleen, lung, kidney, and intestine of the carcass were collected and homogenized in Dulbecco's modified Eagle's medium supplemented with 5% fetal calf serum and 1000 IU of penicillin, 1000 mg of streptomycin, and 10 mg of amphotericin B per ml. Tissue homogenates were clarified by centrifugation at  $2500\times g$  for 10 min.

The fecal samples were immediately examined for common enteric bacterial, protozoan, and viral pathogens, including *Salmonella* spp., *Clostridium* spp., *Campylobacter* spp., shiga-toxin-producing *Escherichia coli* and enterotoxigenic *E. coli*, *Coccidium* spp., *Cryptosporidium* spp., mink Aleutian disease virus [12], MEV [13], CDV [14], caliciviruses [15], rotaviruses [16, 17], coronaviruses [18], and astroviruses [19]. Standardized procedures were carried out to isolate bacteria commonly associated with enteritis *in vitro*. The samples were plated on 5% sheep blood agar (Biocell BioTech., Co., Zhengzhou, China) and cultured aerobically or anaerobically at  $37\text{ }^{\circ}\text{C}$  for 48 h for pathogen detection. Bacteriological investigations were conducted in accordance with standard biochemical procedures, and bacterial strains were identified using the Biolog Microbial ID System (GeneIII, Biolog Inc. USA). Feces or intestinal

contents were examined to detect intestinal parasites by zinc sulfate flotation. Stools and intestinal sections were subjected to Ziehl–Neelsen staining to identify *Cryptosporidium* spp.

DNA/RNA extracts were screened to detect enteric viral pathogens that are common in minks. Tissue homogenates or fecal suspensions of each sample were prepared by diluting the feces in 0.01 M phosphate-buffered saline at a proportion of 1:10 and a pH of 7.2. The suspensions were then vortexed for 30 s and centrifuged at  $1000\times g$  for 15 min. The supernatant (200  $\mu\text{l}$ ) was used for DNA/RNA extraction using a TIANamp Virus DNA Kit (TIANGEN BioTech. Co., Beijing) or TRIzol LS (Gibco-BRL, Life Tech.) in accordance with the manufacturer's protocol. Nucleic acid templates were stored at  $-80\text{ }^{\circ}\text{C}$  until use. Nucleic acid templates were also extracted from healthy mink feces as a negative control. The primers and the PCR and RT-PCR conditions used to detect viral pathogens have been described elsewhere (Table 1).

PCR was performed as described previously to determine the full-length genome sequence of the newly identified MiCV strain, which we have named "HEB15" [20, 21]. The PCR product was analyzed via electrophoresis using an agarose gel and visualized by staining with ethidium bromide. The amplified product from the positive sample was 600 bp long. The complete genome was amplified from the positive sample obtained via PCR using the primers CV-3, CV-4, repF, and repL. The target DNA bands were extracted from the gel using a QIAGEN Gel Extraction Kit in accordance with the manufacturer's instructions. The purified PCR products were cloned into the pMD18-T Simple vector (Takara, Japan), and the plasmids were introduced into *E. coli* DH5a using a standard transformation technique. At least three independent plasmid clones were analyzed, confirmed, and sequenced by Comate BioTech. Co., Changchun, China.

Sequence reads were assembled using SeqMan (DNASTAR Inc., Madison, WI, USA), and the genome sequence of MiCV was analyzed with the aid of NCBI (<http://www.ncbi.nlm.nih.gov>) and EMBL (<http://www.ebi.ac.uk>) analysis tools. Multiple alignments of nucleotide and predicted amino acid sequences were performed and compared with those of other members of the family *Circoviridae*, which were extracted from the GenBank database using ClustalW in MEGA 6.06 [22].

Putative open reading frames (ORFs) were identified using ORF Finder (NCBI; <http://www.ncbi.nlm.nih.gov/gorf/gorf.html>). The nucleotide sequences of different ORFs were aligned with the cognate sequences of the reference MiCV strain DL13 and other CVs through translation-based alignment. The hairpin and stem-loop structures were identified using the mfold web server (<http://unafold.rna.albany.edu/?q=mfold>). Furthermore, direct and inverted repeat sequences within the intergenic regions were determined

**Table 1** Primers used for detection and cloning of mink circovirus

Target virus	Primer name	Primer sequence (5'-3')	Target gene	Ampli-con size (bp)	Annealing temperature (°C)	References
Mink circovirus	F	ATGCCCGTAAGATCGCGAT	Cap	684	54	[20]
	R	GGTACCTTAAGTTTGCTTTGGG				
	CV-F3	GCCCGCTTAAACGGCTCAAACCGC ATTTTC	Partial genome	1547	49	[11]
	CV-R3	TGGGAGGGGCCTGAGGGATTACGT CATACA				
	repF	ACATCAGCGCTAATGAT	Rep	959	49	This study
	repL	GCTAAAATCAAGTGTAGTATC				
Mink enteritis virus	P1	GGATTCTACGGGTACTTTC	VP2	570	52	[13]
	P2	GGTGTGCCACTAGTTCAGTAT				
CDV	CDV1	ACAGGATTGCTGAGGACCTAT	Nucleoprotein	287	59	[14]
	CDV2	CAAGATAACCATGTACGGTGC				
Mink aleutian disease virus	MADF	CTTGTCACGCTACTAGAATGGT	VP2	693	55	[12]
	MADR	AGCTTAAGGTTAGTTTACATGGTT TACT				
Coronaviruses	IN-2deg	5'-GGGDTGGGAYTAYCCHAARTGY GA-3'	Polymerase	452	49	[18]
	IN-4deg	5'-TARCAVACAACISYRTCRTCA-3'				
Caliciviruses	P290d	GATTACTCCASSTGGGAYTCMAC	RdRp	319	48	[15]
	P289d	TGACGATTTTCATCATCMCCRTA				
Astrovirus	MA2	GGCTTACCCACATICCAAA	Polyprotein	387	55	[19]
	MA4	TGGACCCGCTATGATGGCACIAT				
Rotaviruses	Con 2	ATTCGGACCATTTATAACC	VP4	876	50	[16]
	Con 3	TGGCTTCGCCATTTTATAGACA				
	S9-as	ACTTGCCACCAYYTYTTCCAATT	VP7	400	55	[17]
	S9-csv	ATGAATGGTTATGYAAYCCDATGGA				

using an oligonucleotide repeat finder (<http://www.mgs.bionet.nsc.ru/mgs/programs/oligorep/InpForm.htm>).

Phylogenetic trees based on the full-length genome sequence and the nucleotide sequences of replicase and capsid protein genes were constructed in MEGA 6.06 using neighbor-joining method, which provided statistical support with bootstrapping of over 1000 replicates. Other tree-building methods, including maximum parsimony and maximum likelihood, were used to confirm the topology of the neighbor-joining tree.

The following reference CV strains were used in the phylogenetic analysis: MiCV isolate DL13 (NC\_023885.1, from Dalian City, Liaoning Province, China, in 2013), MiCV isolate Hebei (KM586846.1, from Hebei Province, China, in 2013), BatCV 1 (JX863737), BatCV2 (KC339249), BatCV3 (JQ814849.1), PCV-1 (NC\_001944.1), PCV-2 (AY424401), PCV-3 (NC\_031753.1), dogCV (NC\_020904.1), duck CV (DuCV) (NC\_008033.1), goose CV (GoCV, NC\_003410.1), *Cygnus olor* CV (SwCV) (NC\_025247.1), beak and feather disease virus (BFDV) (NC\_001944.1), gull CV (GuCV) (NC\_008522.1), columbid CV (CoCV) (NC\_003054.1),

starling CV (StCV) (NC\_006561.1), finch CV (FiCV) (DQ845075), canary CV (CaCV) (AJ301633), raven CV (RaCV) (NC\_008521.1), barbel CV (BarCV) (GU799606), human feces-associated CV (GQ404856.1), zebra finch CV (KP793918), human feces-associated CV (GQ404856.1), and European catfish CV (JQ011377.1). The distantly related human cyclovirus 1 (HuCyV-1) (KF031465), cyclovirus PKgoat21 (NC\_014927.1), and cyclovirus PK5006 (GQ404844.1) were used as outgroups.

Of the 12 samples tested, 11 (91.7%) were positive for MiCV. No evidence of mixed infection with different pathogens was found in the analyzed samples. The heart, kidney, and gut samples of the deceased mink tested positive in the PCR targeting the replicase gene of MiCV. *E. coli* isolated from the liver of the mink carcass harbored *iutA*, *sfa* virulence genes and were pathogenic to mice.

The complete sequence was deposited in the GenBank database under accession no. KX268345. The complete genome of MiCV strain HEB15 comprises 1753 nucleotides as a covalently closed circular DNA and has a nucleotide composition of 25.50% A, 26.81% T,

28.92% G, and 18.77% C, with a GC content of 47.69%. Sequence comparisons indicated that the genomes of the two MiCV isolates, namely, DL13 and HEB15, exhibited 99.66% nucleotide sequence identity. The HEB15 genome sequence differed from that of DL13 by six nucleotides. The nucleotide sequence alignment was free of deletion or insertion events.

The genome sequence of MiCV isolate HEB15 was compared individually to those of other CVs, and was found to be 20.3% identical to that of CoCV and 66.6% identical to that of BatCV 1. By contrast, MiCV was more closely related to BatCV 1 (66.6% nucleotide sequence identity) than to dogCVs and GoCVs (20.3.1%–55%).

Nucleotide sequence analyses indicated that the MiCV HEB15 strain exhibited a genome organization similar to that of previously characterized CVs, such as pig CVs (PCVs) and BFDV [9, 23]. Sequence features included a distinctive inverted repeat sequence to form a thermodynamically stable stem-loop with a highly conserved nonanucleotide motif TAGTATTAC at its top, where rolling-circle replication (RCR) of the virus DNA strand has been postulated to initiate. Accordingly, the convention for nucleotide numbering and labeling of ORFs has been adopted from previous reports [10]. Thus, the A residue, which is found in the eighth position in the nonamer and lies immediately downstream of the RCR cleavage site, is regarded as nucleotide position 1.

The MiCV genome was found to contain seven ORFs potentially encoding proteins containing more than 50 amino acids. Similar to PCV 1, PCV 2, and BFDV, the MiCV genomes possessed two major ORFs, one in the viral sense orientation (V1, encoding the viral replicase) and one on the complementary strand in the opposite orientation (C1, encoding the capsid protein). Fig. 1 presents the genome locations of the major ORFs in MiCV. The largest ORF, V1, is located at nucleotide position 48–941 and is postulated to encode the replication-associated protein (Rep), with a predicted length of 297 aa. These values were within the range

of 289 amino acids (BFDV) to 317 amino acids (pigeon CV, [PiCV]) observed in other CVs.

The *rep* gene of HEB15 contained one nucleotide mismatch when compared with DL13, and the substitution resulted in a nonsynonymous codon change. The predicted Rep of MiCV shared 42.1% (GuCV) and 79.7% (BatCV 1) amino acid sequence identity with those of other CVs. Pairwise comparisons showed that the amino acid identity levels of the putative V1 ORF product shared by MiCV with BatCV 1 (79.7%), dogCV (54.5%), and swan CV (51.1%) were broadly similar to those with PCVs (46.5%).

A sequence alignment of the putative Rep of MiCV with those of known members of the genus *Circovirus* identified several highly conserved amino acid motifs, including WWDGY (aa 195–199 in MiCV), DDFYGW (aa 208–213), and DRYP (aa 224–227) [24, 25]. A closer examination of the V1 ORF amino acid sequences showed that the amino acid motifs associated with RCR and the P-loop were present in the sequences of MiCV and those of BFDV and PCVs. The motifs related to RCR activity [26] include FTINN, which occurs at aa 13 to 17 in MiCV, and TPHLQG, which appears at aa 49 to 54 in FiCV. CSK is the sequence of the third RCR motif located at aa 91 to 93 in the MiCV Rep. G\*GKS is the fourth motif, which is putatively associated with dNTPase activity [27], at aa 171 to 175 in the MiCV Rep.

The C1 ORFs, which were the putative *cap* genes of MiCV (nt 1032–1715), encode proteins with 270 amino acids. This value was the smallest and was below the range of 289 (BFDV) to 317 amino acids (PiCV) observed in other CVs. The predicted Cap of MiCV shared 20.7% (DuCV) and 45.4% (PCV 2 and BatCV) amino acid identity with those of other CVs. In addition to the high level of identity shared by PCV 2 and BatCV (45.4%), the highest amino acid sequence identity was shared by PCV 1 (43.6%). MiCV also shared higher levels of identity with mammalian CVs, such as PCVs (43.6% and 45.4%) and BatCV 1 (45.4%), than with avian CVs (20.7%–26.0%). Similar to other animal CVs,

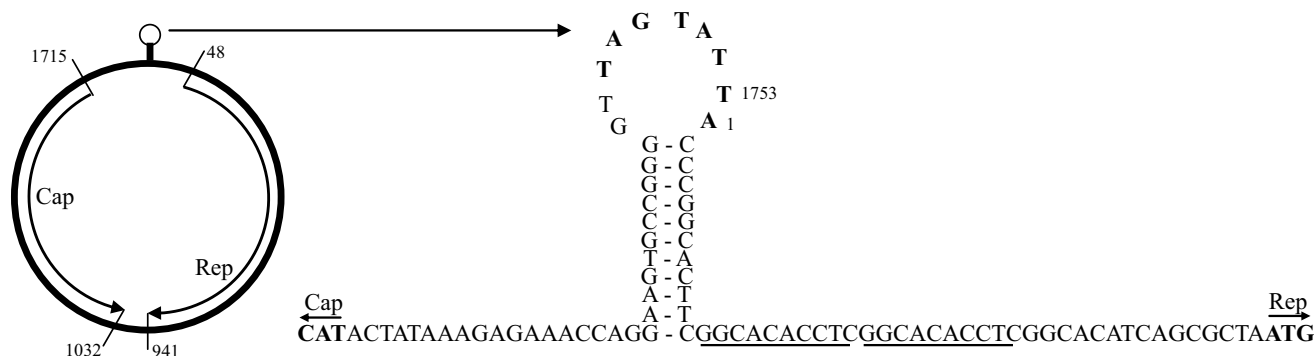


**Fig. 1** Diagram of the circovirus genome isolated from mink. The nucleotide position is indicated for each ORF. Rep, replicase; Cap, capsid protein. The hairpin-like palindromic structure, the origin of replication, is shown on the right

MiCV had a putative capsid protein with an amino terminus containing an arginine (R)-rich stretch with a length of 30 aa.

The *cap* nucleotide sequences of MiCV HEB15 and the two other strains of MiCV, namely, DL13 and Hebei13, were 99.3% and 99.7% identical, respectively. Furthermore, a high degree of identity (99.3%–99.7%) was observed between the nucleotide sequences of MiCV strains. The *cap* gene contained five nucleotide mismatches compared with the DL13 isolate. Three of the five substitutions were transversions, and all of the substitutions resulted in nonsynonymous codon changes. The alignment of the entire Cap protein sequence of MiCV HEB15 with the published sequences of DL13 and Hebei13 indicated that the sequences were generally highly conserved, showing no variation at all. Moreover, the five nucleic acid substitutions did not result in changes in amino acids.

Database searches with the MiCV sequence revealed that none of the minor ORFs shared significant amino acid sequence similarity with any of the ORFs specified by other CVs. However, a putative ORF, postulated to use an alternative TTG start codon, occurred on the complementary strands (nt 887–504), which shared weak homology with the C2 ORF of DuCV (26%) and was in a similar location to those of previously characterized CVs.

Like other CVs, the HEB15 genome was found to contain two intergenic noncoding regions located between the replicase and the capsid protein genes (Table 2). The 5' and 3' intergenic regions of MiCV were 85 and 90 nt in length, respectively (Table 2). In the 5' intergenic region of MiCV, the conserved nonanucleotide motif of MiCV was flanked by

a potential stem-loop with 11 base pairs in the stem. In addition, the intergenic region of MiCV possessed two tandemly repeated decamers GGCACACCTC (nt 13–22 and 23–32) adjacent to the potential stem-loop. In the 3'-intergenic region, a 45-nt stretch within the 3' intergenic sequence showed 97.78% (44/45) nt sequence identity to its counterpart in BatCV 1 (isolate XOR), which was recently detected in bats by metagenomic analysis of tissue samples [28].

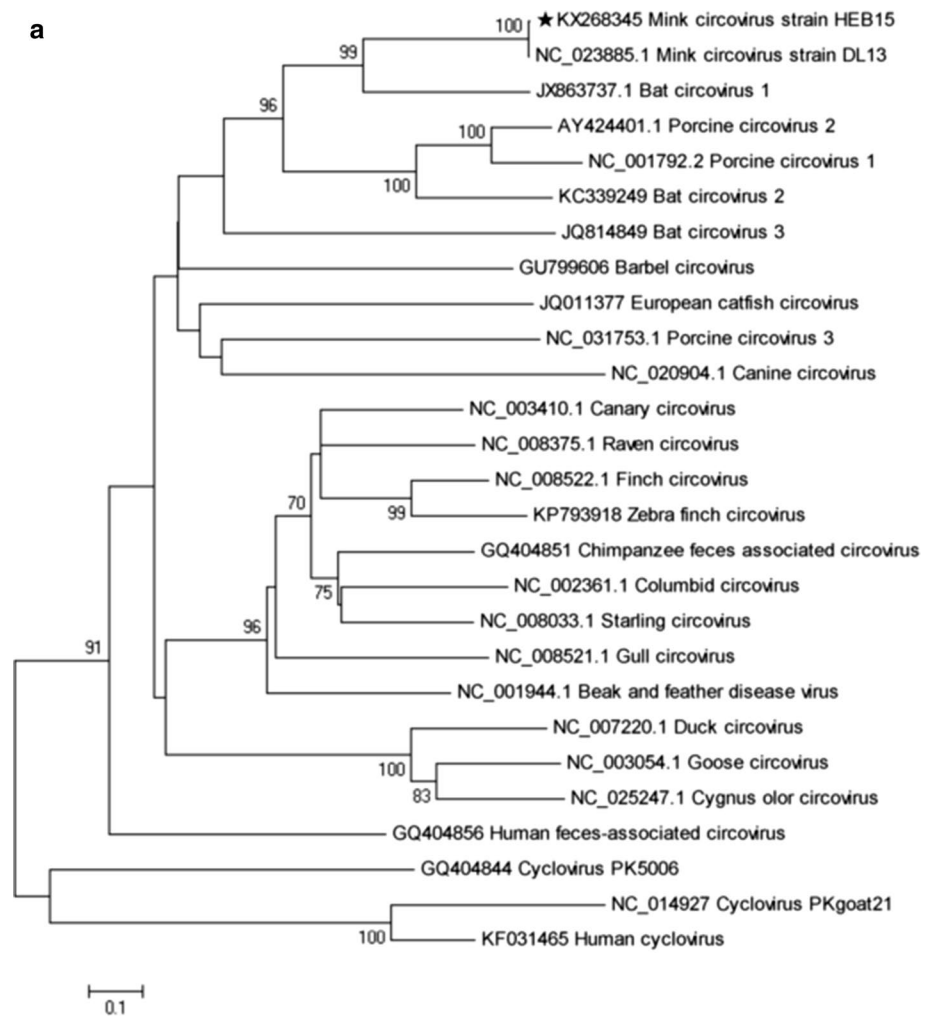
Potential poly(A) signals appropriately located for use with possible transcripts containing the V1 and C1 ORFs were identified in the MiCV genomes by analogy to similar sequences in the PCV and BFDV genomes [23, 24]. Potential poly(A) signals for the V1 ORF were determined at nt 924–929 (AATAAAA) and nt 937–943 (ATTAATA). In the complementary strand, three possible signals for the C1 ORF were identified at nt 944–950 (AATAAAA), nt 961–968 (GATAAAA), and nt 1030–1036 (CTTAATA).

A phylogenetic analysis based on the complete genome sequences of the two MiCV strains and representative CVs was performed to investigate the genetic relationship between MiCV and other CVs (Fig. 2). In the neighbor-joining tree, the MiCV strains were grouped with mammalian CV, which comprised BatCV 1, dogCV, and PCVs, and these were clearly separated from bird CVs. MiCVs were more closely related to PCV 1 and PCV 2 than to dogCV (Fig. 2a). A phylogenetic analysis based on *rep* sequences (Fig. 2b) demonstrated that the two MiCV strains were grouped with BatCVs and were more closely related to dogCV than to PCV 1 and PCV 2. In trees constructed based on the *cap* gene, the MiCVs were tightly intermingled with BatCV 1 isolate and were close to PCV 1 and PCV 2, but dogCV

**Table 2** Summary of data relating to genome features of circoviruses

Virus	Genome length (nucleotides)	Length of 5' intergenic region (nucleotides)	Length of 3' intergenic region (nucleotides)	Nonanucleotide sequence	Tandem repeat motif	Cap protein length (amino acids)	Rep protein length (amino acids)
MiCV	1753	85	90	TAGTATTAC	GGCACACCTC	227	297
PCV1	1759	82	36	TAGTATTAC	CGGCAGC	233	312
PCV2	1768	83	38	AAGTATTAC	CGGCAGCAC CTC	233	314
BFDV	1993	145	234	TAGTATTAC	GGGGCACCG	247	289
PiCV	2037	90	171	TAGTATTAC	GGACCCAC	273	317
CaCV	1952	77	249	CAGTATTAC	GGAGCCAC	250	290
FiCV	1962	71	307	TAGTATTAC	TGGAACC	249	291
GuCV	2035	207	72	TAGTATTAC	GGGGCCAT	245	305
GoCV	1821	132	54	TATTATTAC	GTACTCCG	250	293
DuCV	1996	111	232	TAGTATTAC	TACTCCG	257	292
DogCV	2063	135	203	TAGTATTAC	CACAG	270	303
BatCV	1862	86	171	TAGTATTAC	CACTTCGGCA	238	295
StCV	2063	79	293	CAGTATTAC	GGAGCCA	276	289
SwCV	1783	107	39	TATTATTAC	ACTAC	251	293
RaCV	1898	86	204	GAGTATTAC	GGAGCC	243	291

**Fig. 2** Phylogenetic analysis of the genome sequences of mink circovirus and other circoviruses, using the neighbor-joining method, with 1,000 bootstrap replicates (MEGA 6.06). **a** Analysis of the whole genome sequence. **b** Analysis of the rep gene sequence. **c** Analysis of the cap gene sequence. Only bootstrap support values greater than 60% are shown. The bar indicates the genetic distance. The sequence of the circovirus isolated in this study is indicated by a star. Other sequences were obtained from GenBank; accession numbers of those sequences are included in the tree



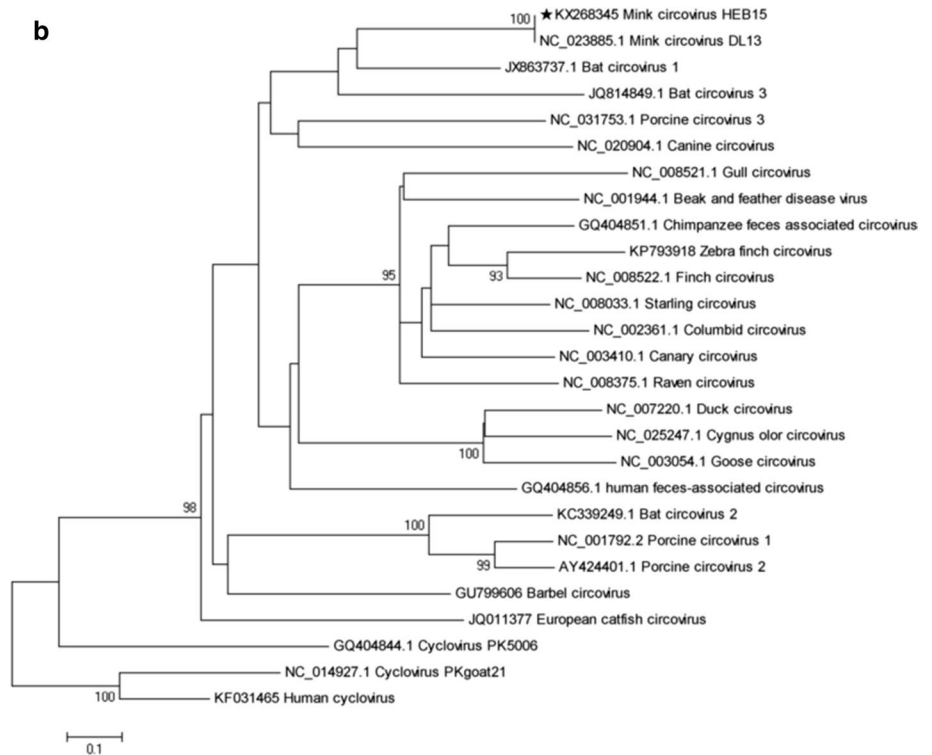
was grouped into a separate cluster (Fig. 2c). These results were verified using the maximum-likelihood and maximum-parsimony methods, which yielded the same tree topology (data not shown).

MiCV circulated on mink farms in Dalian City, Liaoning Province, China, in 2013 [11]. Farmers observed disease in MEV-vaccinated minks in 1978. Clinical signs included diarrhea, lethargy, anorexia, pale muzzle, and unkempt fur. On farms with diseased minks, all of the animals were affected, and 70%–80% showed clinical signs. However, most of the animals recovered, and fewer than 10% of the affected minks died. MiCV was found in the liver, digestive tract, and fecal specimens of minks and was shown to be responsible for diarrhea [11]. However, its pathogenic role remains unknown, particularly its infection or coinfection process. In the present study, we investigated a major outbreak in a large population. Samples were tested for other causative agents, including MADV, MEV, CDV, coronavirus, calicivirus, rotavirus, bacterial pathogens, and parasites. After these pathogens were excluded, MiCV was detected alone, and was not found in combination with other key

pathogens, such as MADV, MEV, and CDV. Thus, our findings suggested a possible association between MiCV and mink acute enteritis. Consistent with the detection results presented by Lian et al. [11], our findings showed that the virus was located in the gut and feces. The virus was also found in the heart and kidney, but not in the liver.

The sites where carcasses and feces were collected in this study were approximately 1000 km away from where Lian et al. obtained their samples [11], and the isolates were therefore of different geographical origin. Moreover, the mink breed, disease symptoms, and disease duration differed. As such, the sustained direct transmission of MiCV among minks was excluded, and MiCV HEB15 was considered a new strain. The data gathered in this study expanded the known geographical distribution of MiCV. Unfortunately, the carcass of the MiCV-infected mink was not stored properly by the resident veterinarians and underwent repeated cycles of freezing and thawing, making it unsuitable for histopathological examination. For this reason, valuable information on tissue localization and alterations of MiCV could not be collected. The present study could contribute

Fig. 2 (continued)



to our knowledge of the pathogenic potential of MiCV and its association with mink enteritis if our results were corroborated by further reports. The presence of MiCV might help to explain the different disease outcomes and severity often observed in MADV-/MEV-infected animals. Our results indicate that minks with acute gastroenteritis should be screened for MiCV and established pathogens, such as *E. coli* and MEV. This study was conducted to identify the viral agents associated with acute diarrhea in minks, and no attempt was made to determine the primary cause of death.

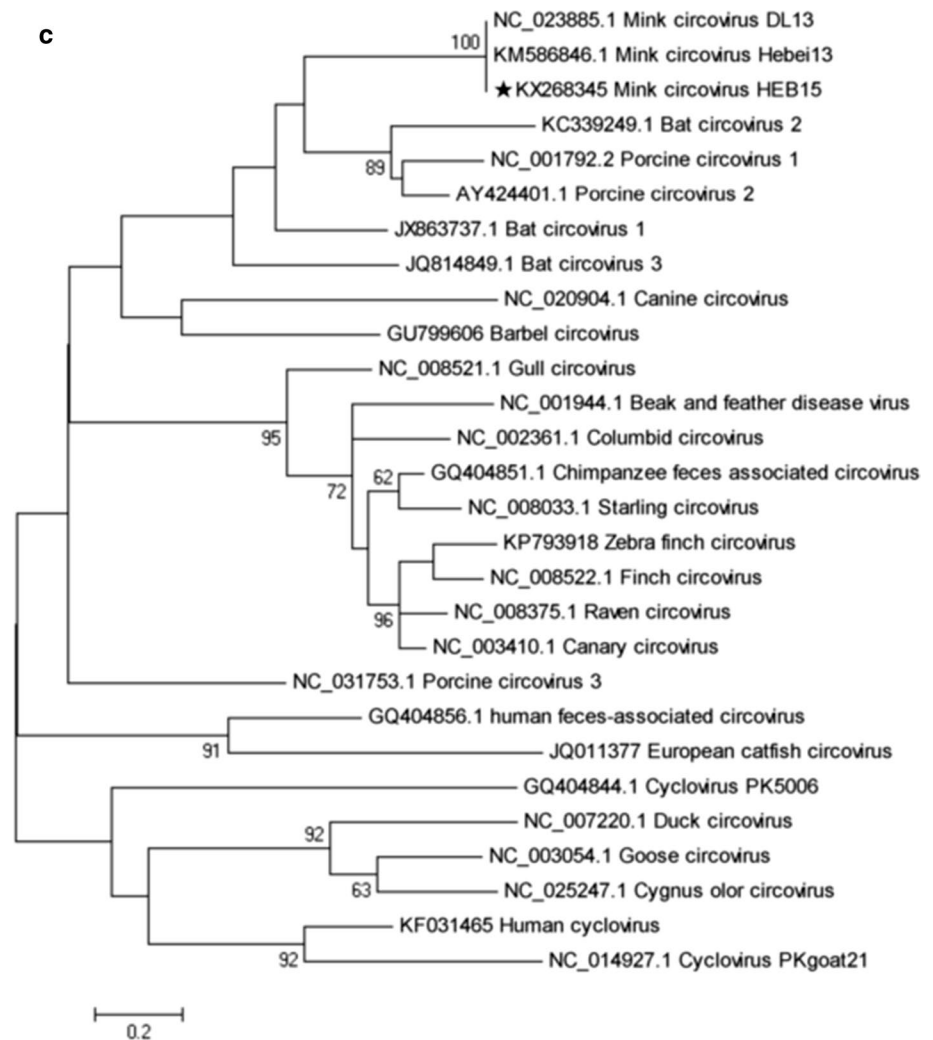
To date, attempts to isolate MiCV have been unsuccessful. Current surveillance methods are limited to viral detection using molecular assays, and no seroprevalence information is available. As a consequence, the identification and characterization of the virus depends on genetic approaches such as PCR and sequence determination and analysis. In this study, the nucleotide sequence of the MiCV genome was determined and analyzed. Our results showed that the genome sequence of MiCV isolate HEB15 was highly similar to that of MiCV DL13 in terms of size (1753 nt), nucleotide sequence (99.66% identity), and ORF analysis. The examination of other MiCV sequences from different regions will help to assess the level of genetic diversity. In our study, sequence analysis confirmed that MiCV genomes displayed the characteristics of members of the genus *Circovirus*, and the common features included their genome organization, the presence of a potential stem-loop and conserved nonanucleotide motif

postulated to be the origin of viral DNA replication, and major ORFs and repeats [26, 27]. Conserved amino acid motifs, including WWDGY, DDFYGLWP, and DRYP, which have unknown functions, were also recognized within Rep associated with RCR and dNTPase activity. These motifs could be utilized to design primers that could amplify CV-specific DNA for discovery of new CVs in other hosts.

Additional MiCV surveillance in animals is required to clarify CV epidemiology. Further efforts are necessary to identify and characterize the infection or coinfection processes. Future studies should investigate experimental infections to obtain conclusive information on the pathogenic role of MiCV and to monitor the circulation of these viruses and their effects on mink populations.

This study could contribute to our knowledge about the pathogenic potential of MiCV and its association with acute gastroenteritis in minks. The complete genome sequence of MiCV strain HEB15 is reported here to help elucidate the epidemiological, evolutionary, and pathogenic characteristics of mammalian CVs. The availability of the MiCV genome sequence also provides a basis for the development of molecular reagents that could be used to identify other novel CVs that infect other mammalian species.

Fig. 2 (continued)



**Acknowledgements** We acknowledge the valuable help provided by Prof. Wei Li of Northeast Agricultural University.

**Funding** This work was supported by National Natural Science Foundation of China (No. 31101845), the Natural Science Foundation of Heilongjiang Province (LC2015006) and State Key Laboratory of Veterinary Biotechnology Foundation (SKLVB201611).

### Compliance with ethical standards

**Conflict of interest** The authors declare no conflicts of interest.

**Ethical approval** This article does not contain any studies with human participants performed by any of the authors. This study was performed in accordance with the recommendations in the Guide for the Care and Use of Laboratory Animals of the Ministry of Health, China. Prior to experiments, the protocol of the current study was reviewed and approved by the Institutional Animal Care and Use Committee of Northeast Agricultural University (approved protocol number 2014-

SRM-25). Samples were collected only from animals for laboratory analyses, avoiding unnecessary pain and suffering of the animals. The mink owners gave their written consent for necropsy and sample collection.

### References

- Breitbart M, Delwart E, Rosario K, Segalés J, Varsani A; ICTV Report Consortium (2017) ICTV virus taxonomy profile: *Circoviridae*. J Gen Virol 98(8):1997–1998
- Li L, Sabrina MG, Zhu K, Leutenegger CM, Marks SL, Steven K, Patricia G, Dela CJFN, Wang C, Eric D (2013) Circovirus in tissues of dogs with vasculitis and hemorrhage. Emerg Infect Dis 19(4):534–541
- Decaro N, Martella V, Desario C, Lanave G, Circella E, Cavalli A, Elia G, Camero M, Buonavoglia C (2014) Genomic characterization of a circovirus associated with fatal hemorrhagic enteritis in dog, Italy. PLoS One 9(8):e105909



4. Segalés J (2012) Porcine circovirus type 2 (PCV2) infections: clinical signs, pathology and laboratory diagnosis. *Virus Res* 164(2):10–19
5. Todd D (2004) Avian circovirus diseases: lessons for the study of PMWS. *Vet Microbiol* 98(2):169–174
6. Woods LW, Latimer KS, Barr BC, Niagro FD, Campagnoli RP, Nordhausen RW, Castro AE (1993) Circovirus-like infection in a pigeon. *J Vet Diagn Investig* 5(4):609–612
7. Shivaprasad HL, Chin RP, Jeffrey JS, Latimer KS, Nordhausen RW, Niagro FD, Campagnoli RP (1994) Particles resembling circovirus in the bursa of Fabricius of pigeons. *Avian Dis* 38(3):635–641
8. Todd D, McNulty MS, Adair BM, Allan GM (2001) Animal circoviruses. *Adv Virus Res* 57:1–70
9. Finsterbusch T, Mankertz A (2009) Porcine circoviruses—small but powerful. *Virus Res* 143(2):177–183
10. Todd D (2000) Circoviruses: immunosuppressive threats to avian species: a review. *Avian Pathol* 29(5):373–394
11. Lian H, Liu Y, Li N, Wang Y, Zhang S, Hu R (2014) Novel circovirus from mink, China. *Emerg Infect Dis* 20(9):1548–1550
12. Oie KL, Durrant G, Wolfenbarger JB, Martin D, Costello F, Perryman S, Hogan D, Hadlow WJ, Bloom ME (1996) The relationship between capsid protein (VP2) sequence and pathogenicity of Aleutian mink disease parvovirus (ADV): a possible role for raccoons in the transmission of ADV infections. *J Virol* 70(2):852
13. Wang J, Cheng S, Yi L, Cheng Y, Yang S, Xu H, Li Z, Shi X, Wu H, Yan X (2013) Detection of mink enteritis virus by loop-mediated isothermal amplification (LAMP). *J Virol Methods* 187(2):401–405
14. Saito TB, Alfieri AA, Wosiacki SR, Negrão FJ, Morais HSA, Alfieri AF (2006) Detection of canine distemper virus by reverse transcriptase-polymerase chain reaction in the urine of dogs with clinical signs of distemper encephalitis. *Res Vet Sci* 80(1):116–119
15. Jiang X, Huang PW, Zhong WM, Farkas T, Cubitt DW, Matson DO (1999) Design and evaluation of a primer pair that detects both Norwalk- and Sapporo-like caliciviruses by RT-PCR. *J Virol Methods* 83(1–2):145–154
16. Gentsch JR, Glass RI, Woods P, Gouvea V, Gorziglia M, Flores J, Das BK, Bhan MK (1992) Identification of group A rotavirus gene 4 types by polymerase chain reaction. *J Clin Microbiol* 30(6):1365–1373
17. Schumann T, Hotzel H, Otto P, Johne R (2009) Evidence of inter-species transmission and reassortment among avian group A rotaviruses. *Virology* 386(2):334–343
18. Vlasova AN, Halpin R, Wang S, Ghedin E, Spiro DJ, Saif LJ (2011) Molecular characterization of a new species in the genus Alphacoronavirus associated with mink epizootic catarrhal gastroenteritis. *J Gen Virol* 92(Pt 6):1369–1379
19. Mittelholzer C, Hedlund KO, Englund L, Dietz HH, Svensson L (2003) Molecular characterization of a novel astrovirus associated with disease in mink. *J Gen Virol* 84(11):3087–3094
20. Wang Y, Liu Y, Lian H, Li N, Zhang L, Hu R (2015) Molecular epidemiology of mink circovirus. *Chin J Vet Med* 51:6–8
21. Junwei G, Baoxian L, Lijie T, Yijing L (2006) Cloning and sequence analysis of the N gene of porcine epidemic diarrhea virus LJB/03. *Virus Genes* 33(2):215–219
22. Tamura K, Stecher G, Peterson D, Filipinski A, Kumar S (2013) MEGA6: molecular evolutionary genetics analysis version 6.0. *Mol Biol Evol* 30(12):2725–2729
23. Bassami MR, Berryman D, Wilcox GE, Raidal SR (1998) Psittacine beak and feather disease virus nucleotide sequence analysis and its relationship to porcine circovirus, plant circoviruses, and chicken anaemia virus. *Virology* 249(2):453–459
24. Todd D, Weston JH, Soike D, Smyth JA (2001) Genome sequence determinations and analyses of novel circoviruses from goose and pigeon. *Virology* 286(2):354–362
25. Stewart ME, Perry R, Raidal SR (2006) Identification of a novel circovirus in Australian ravens (*Corvus coronoides*) with feather disease. *Avian Pathol* 35(02):86–92
26. Ilyina TV, Koonin EV (1992) Conserved sequence motifs in the initiator proteins for rolling circle DNA replication encoded by diverse replicons from eubacteria, eucaryotes and archaeobacteria. *Nucleic Acids Res* 20(13):3279–3285
27. Desbiez C, David C, Mettouchi A, Laufs J, Gronenborn B (1995) Rep protein of tomato yellow leaf curl geminivirus has an ATPase activity required for viral DNA replication. *Proc Natl Acad Sci USA* 92(12):5640–5644
28. He B, Li Z, Yang F, Zheng J, Feng Y, Guo H, Li Y, Wang Y, Su N, Zhang F (2013) Virome profiling of bats from Myanmar by metagenomic analysis of tissue samples reveals more novel mammalian viruses. *PLoS One* 8(4):e61950